

Molecular and electronic structures of acryloyl isothiocyanate, CH₂CHC(O)NCS: a joint experimental and theoretical study†

Maofa Ge,^{*a} Chunping Ma,^{ab} Shengrui Tong,^{ab} Wei Xue,^{ab} Zhifeng Pu^a
and Dianxun Wang^a

Received (in Victoria, Australia) 1st April 2009, Accepted 24th June 2009

First published as an Advance Article on the web 28th July 2009

DOI: 10.1039/b906486a

Acryloyl isothiocyanate, CH₂CHC(O)NCS, was prepared and studied by IR, Raman, photoelectron spectroscopy (PES), photoionization spectroscopy (PIMS) and theoretical calculations. This molecule was theoretically predicted to prefer the *trans-cis* (tc) conformation as the most stable conformer, with the CO bond *trans* to the CC bond and *cis* to the NCS group. IR and Raman spectra also suggest the presence of the tc conformation only. A theoretical study involving the calculation of the ionization energies using the orbital valence Green's functional (OVGF/6-311 + G(d)) was performed to aid the assignment of the PE spectrum. The first vertical ionization energy of CH₂CHC(O)NCS was determined to be 9.89 eV, which is mainly the ionization of the out-of-plane bonding π_{NCS} orbital. Natural population analysis (NPA and NBO) were also performed to investigate the reactivity of CH₂CHC(O)NCS.

Introduction

Recently, research interest in isothiocyanates has become more intense because of their wide variety of medicinal, pharmacological and industrial applications.^{1–5} Their reactions, which take place *via* nucleophile attack on the carbon of NCS group, give high yields and exhibit no side reactions; they are also examples of distorted linear triatomic systems. The distortions of the NCS moiety from linearity have been investigated in some detail.⁶ The –NCS π -system contained in cruciferae plants and vegetables give them a particular flavor and most importantly causes them to possess a number of interesting medicinal properties.^{7–9} In particular, isothiocyanates inhibit the medicinal proliferation of tumor cells both *in vitro* and *in vivo*, and are used as chemopreventive agents.^{10–13} The initiating event for these effects seems to be acute cellular stress caused by this class of compounds, although the elucidation of the mechanism is still at an early stage. Furthermore, due to their volatility, these compounds can reach the troposphere and react with radicals to give certain conversion products, thereby presenting an ecological risk.¹⁴

Many of these behavioural phenomena are undoubtedly related to their electronic structures.¹⁵ However, the influence of electronic structure on the chemical behavior of these species is not yet properly characterized, a better understanding of which may help to find them further applications.¹⁶ These compounds were investigated previously by UV photoelectron spectroscopy (UPS) and MO calculations. Little experimental

data has been reported in the literature on the electronic structure of isothiocyanates. Derivatives studied previously include alkyl isothiocyanates,¹⁷ methyl isothiocyanates,^{18–20} silicon isothiocyanates,^{16,21} halogen thiocyanates²² and aromatic isothiocyanates.⁶ Considering the information that has been reported, we were interested in the electronic structure of the corresponding acryloyl isothiocyanate.

Here, we present the results of our photoelectron spectroscopy and photoionization mass spectroscopy studies of acryloyl isothiocyanate, CH₂CHC(O)NCS, for the first time and determine its ionization energies, as well as elucidating the corresponding valence electronic structures on the basis of theoretical calculations. To form a comparison with the experimental ionization values, a complete theoretical study, involving structure calculations of stable conformers at different levels of theory, was performed. MO analysis and ionization energy calculations were also carried out.

Results and discussion

The geometry of CH₂CHC(O)NCS

Isothiocyanates are rather intriguing compounds, since the SCN group is ambidentate, bonding at either S or N and forming R–S–C \equiv N (thiocyanate)- or R–N=C=S (isothiocyanate)-type molecules.²³ The parent acid exists as HNCS in the gas phase, whereas both methyl derivatives,²⁴ CH₃NCS and CH₃SCN,²⁵ can be isolated, as well as CH₂CHNCS and CH₂CHSCN.²⁶ The halogen thiocyanates, on the other hand, are known only as unstable intermediates in solution; chemical and spectroscopic studies indicate an XSCN rather than an XNCS structure.^{22,27–29} This is also the case for the selenium analogues RSeCN (X = Cl, Br,³⁰ I,³¹ CN³⁰ and CH₃OC(O)S³²). This is in contrast to the substituted oxygen analogues XNCO (X = CN,³³ Cl, Br, I,³⁴ CH₃C(O)³⁵ and CH₃OC(O)S^{36,37}), which bond only through nitrogen. As for the acryloyl

^a Beijing National Laboratory for Molecular Sciences (BNLMS), State Key Laboratory for Structural Chemistry of Unstable and Stable Species, Beijing, 100190, China. E-mail: gemaofa@iccas.ac.cn

^b Graduate School of Chinese Academy of Sciences, Beijing, 100049, China

† Electronic supplementary information (ESI) available: Data Tables S1 and S2. See DOI: 10.1039/b906486a

derivative, hardly any experimental or theoretical studies on its structural and spectroscopic properties have been reported so far, and only the $\text{CH}_2\text{CHC}(\text{O})\text{NCS}$ form was found in our experimental investigations. Therefore we have just studied the geometry of $\text{CH}_2\text{CHC}(\text{O})\text{NCS}$ here. Generally, several conformations are feasible, depending on the orientation around the C–C and C–N single bonds. The molecular structure and conformational properties of related $\text{CH}_2\text{CHC}(\text{O})\text{Cl}$ and $\text{CH}_3\text{C}(\text{O})\text{NCS}$ had been studied by theoretical and experimental methods.^{35,38} The previous vibrational and theoretical investigations indicate that the *trans* conformation is preferred for acryloyl chloride and the *trans-cis* ($\Phi_{\text{C}=\text{C}-\text{C}=\text{O}} = 180^\circ$, $\Phi_{\text{O}=\text{C}-\text{N}=\text{C}} = 0^\circ$) conformation is preferred for acryloyl isocyanate in the gas phase,³⁹ while substantial amounts of both conformers are present in the condensed phase. According to these antecedents, the structure of $\text{CH}_2\text{CHC}(\text{O})\text{NCS}$ with both *syn*-periplanar orientations around the CC and CN single bonds was used as the initial form in the calculations. To gain insight into the conformational preference of this molecule, the potential energy functions for internal rotation around the $\Phi_{\text{C}=\text{C}-\text{C}=\text{O}}$ and $\Phi_{\text{O}=\text{C}-\text{N}=\text{C}}$ dihedral angles were calculated at the MP2/6-311+G* level by allowing geometry optimizations, with the respective dihedral angles, Φ , varying from 0 to 360° in steps of 10° . The potential energy curves are shown in Fig. 1.

As seen from Fig. 1, four conformers are predicted to be stable structures. As expected for the $\text{CH}_2\text{CHC}(\text{O})$ moiety, a *trans* orientation of $\Phi_{\text{C}=\text{C}-\text{C}=\text{O}}$ dihedral angle is preferred, given that the *cis* form is higher in energy. Likewise, four structures correspond to minima in the potential energy curve around the $\Phi_{\text{O}=\text{C}-\text{N}=\text{C}}$ dihedral angle. The most stable one shows a *cis* orientation of the CO and NC bonds, while the *trans* form is higher in energy. Similarly, the resulting potential energy curve for the rotation of the $\Phi_{\text{O}=\text{C}-\text{N}=\text{C}}$ dihedral angle possesses minima for three planar forms and one non-planar form, and the non-planar form possesses the highest energy and the least stability.

Moreover, full geometry optimizations and frequency calculations for the four feasible conformers have been

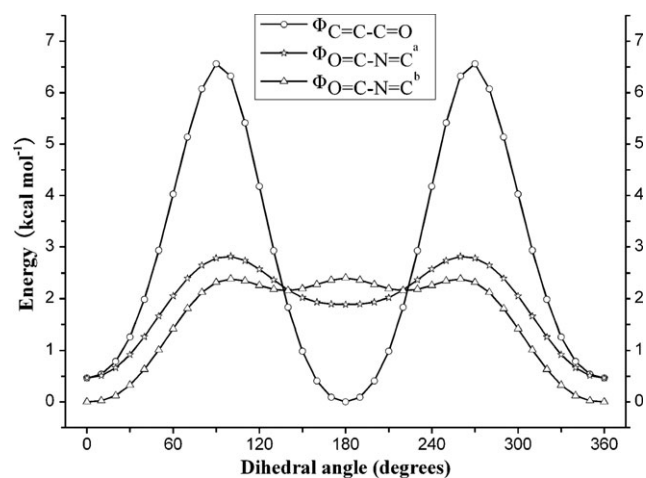


Fig. 1 Potential energy curves of $\text{CH}_2\text{CHC}(\text{O})\text{NCS}$ by rotating the C–C and C–N bonds from 0 to 360° in steps of 10° (^a $\Phi_{\text{C}=\text{C}-\text{C}=\text{O}} = 0^\circ$, ^b $\Phi_{\text{C}=\text{C}-\text{C}=\text{O}} = 180^\circ$).

Table 1 Calculated relative energies (/kcal mol^{−1}) of different conformers of $\text{CH}_2\text{CHC}(\text{O})\text{NCS}$

	tc	cc	ct	tt
B3LYP/6-311++G(3df,3pd)	0.0	0.34	1.53	1.90
B3P86/6-311++G(3df,3pd)	0.0	0.47	1.49	1.72
B3PW91/6-311++G(3df,3pd)	0.0	0.42	1.47	1.79
MP2/6-311++G**	0.0	0.59	1.75	2.25

performed using three DFT methods (B3LYP, B3P86 and B3PW91) and the 6-311++G(3df,3pd) basis set; single point energies were calculated at the MP2/6-311++G** level. Relative ΔE energy values are listed in Table 1. All computational methods predict a structure with a *trans* C=C=O orientation and a *cis* O=C–N=C orientation to be the most stable conformer of $\text{CH}_2\text{CHC}(\text{O})\text{NCS}$ (tc). The second stable form, higher in energy by 0.59 kcal mol^{−1} (MP2/6-311++G**), corresponds to a conformer with a *cis* orientation around the two dihedral angles (cc). A third conformer, named *cis-trans* (ct) in Fig. 2, with a *trans* orientation of the C=O and N=C bonds, becomes a minima in the potential hypersurface as well, located at 1.75 kcal mol^{−1} above the global minimum. The calculated energy of the fourth conformer, with a *trans* orientation of both dihedral angles (tt), is higher than 2.25 kcal mol^{−1} with respect to the minimum (Table 1). Furthermore, for acryloyl isothiocyanate, the rotational barrier from tc to cc was predicted to be 6.56 kcal mol^{−1}, and it is smaller than that of acryloyl isocyanate (7.84 kcal mol^{−1}).³⁹ Compared with other saturated analogues, we found that the rotation around the C–C or C–N single bond is less hindered with relatively low energetic barriers due to π -conjugation.⁴⁰

Selected geometric parameters obtained by the B3LYP/6-311++G(3df,3pd) approach for the most stable conformer and the radical cation form for $\text{CH}_2\text{CHC}(\text{O})\text{NCS}$ are given in Table 2. Apparent changes can be found in the bond lengths and angles between the neutral molecule and the radical cation form. The most significant change is the C–N bond length, which elongates from 1.417 to 1.458 Å after ionization. This is similar to that of acetyl isothiocyanate, whose C–N bond elongates from 1.424 to 1.533 Å. Contrary to the corresponding isocyanate, the C–N single bond shortens (from 1.428 to 1.346 Å) after ionization.³⁹ Similar to acetyl isothiocyanate, the C=O

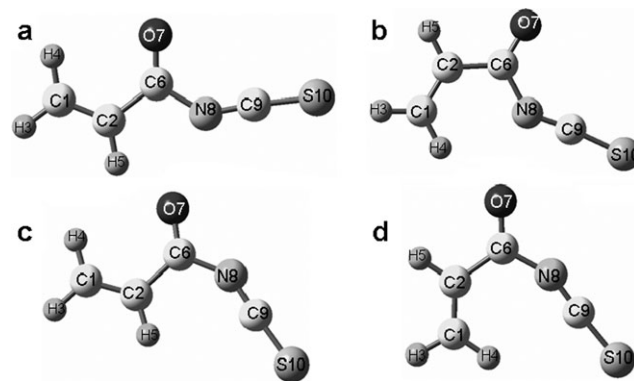


Fig. 2 A schematic representation of the four conformers of $\text{CH}_2\text{CHC}(\text{O})\text{NCS}$: (a) *cis-cis* (cc), (b) *trans-cis* (tc), (c) *cis-trans* (ct) and (d) *trans-trans* (tt).

Table 2 Calculated geometric parameters for the tc conformer of $\text{CH}_2\text{CHC}(\text{O})\text{NCS}^a$ and for its radical cation form, $\text{CH}_2\text{CHC}(\text{O})\text{NCS}^{*+}$, calculated by different methods at the 6-311++G(3df,3pd) basis set level

Parameters	Neutral			Cation B3LYP
	B3PW91	B3P86	B3LYP	
γ_{C1C2}	1.329	1.327	1.329	1.335
γ_{C2C6}	1.471	1.468	1.473	1.441
γ_{C6O7}	1.203	1.202	1.204	1.198
γ_{C6N8}	1.412	1.411	1.417	1.458
γ_{N8C9}	1.203	1.203	1.204	1.193
γ_{C9S10}	1.557	1.555	1.561	1.572
α_{C1C2C6}	124.0	123.8	124.3	121.9
α_{C2C6O7}	123.7	123.7	123.6	130.6
α_{C2C6N8}	114.5	114.4	114.6	117.9
α_{O7C6N8}	121.8	121.9	121.8	111.4
α_{C6N8C9}	138.6	138.2	138.2	148.4
α_{N8C9S10}	175.6	175.7	175.8	175.6
δ_{C1C2C6O7}	180.0	180.0	180.0	180.0
δ_{O7C6N8C9}	0.0	0.0	0.0	0.0
$\delta_{\text{C6N8C9S10}}$	180.0	180.0	180.0	177.0

^a Values are given in Å and °. For atom numbering, see Fig. 2.

bond length shortens from 1.204 to 1.198 Å, and the C–C=O and O=C–N angles change from 123.6 and 121.8 to 130.6 and 111.4°, respectively. In addition, the dihedral angle $\delta_{\text{C6N8C9S10}}$ changes from 180 to 177.0° after ionization, which is completely different to that of acetyl isothiocyanate and acryloyl isocyanate.^{35,39}

Vibrational analysis

No experimental or theoretical calculations have been reported for $\text{CH}_2\text{CHC}(\text{O})\text{NCS}$. Fig. 3 presents the IR (gas) and Raman (liquid) spectra of $\text{CH}_2\text{CHC}(\text{O})\text{NCS}$. Experimentally observed vibrational data are collected, together with the theoretically predicted wavenumbers (B3LYP/6-311++G(3df,3pd)) for the most stable conformer and tentative assignments are given in the ESI (Table S1).† The vibrational modes were assigned in comparison with the theoretical wavenumbers and intensities, as well as with relevant reported data, specially of $\text{CH}_2\text{CHC}(\text{O})\text{Cl}$,⁴¹ $\text{CH}_3\text{C}(\text{O})\text{NCS}$ ⁴² and CH_2CHNCS .⁴³ This molecule in its planar tc conformation possesses C_s symmetry. Thus, in $\text{CH}_2\text{CHC}(\text{O})\text{NCS}$, the $3N - 6 = 24$ normal modes of vibration correspond to an irreducible representation $17A' + 7A''$ for the in-plane and out-of-plane modes, respectively.

Generally, the *ab initio* and DFT harmonic vibrational frequencies are overestimated.⁴⁴ Since this overestimation is found to be consistent, the constant or exponential scaling method is often employed.⁴⁵ Due to the similar energies of the tc and cc conformers, it is possible that a second stable cc form may also exist with the tc form at ambient temperature, but that the main conformer is the latter in the gas phase. Furthermore, it was found that the experimental IR spectrum was in more agreement with the theoretical spectrum of the tc conformer (see the ESI, Table S1†). For simplicity, our discussion is reduced to the analysis of the energetically more favorable tc conformer.

All of the stretching modes at high wavenumbers are characteristic and easily assignable. The carbonyl and NCS

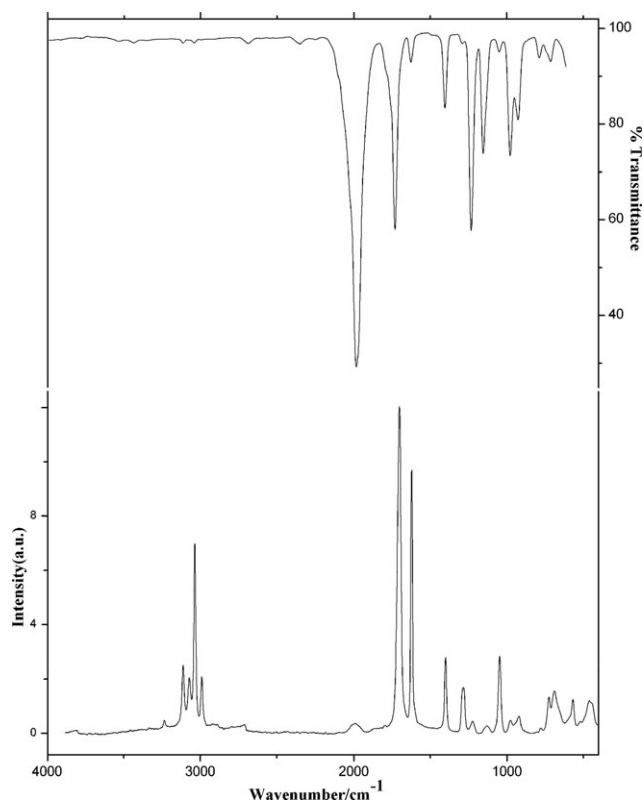


Fig. 3 The gas phase IR spectrum (top) and liquid phase Raman spectrum (bottom) of $\text{CH}_2\text{CHC}(\text{O})\text{NCS}$.

stretching vibrations give rise to three prominent IR absorptions.⁴² The NCS antisymmetric stretching mode appears only as a very weak and broad line in the Raman spectrum. The strong 1980–2100 and 450–700 cm^{-1} IR features are diagnostic of isothiocyanates, being rather insensitive to the nature of the substituents.^{42,43,46} The characteristic vibrational frequencies of the vinyl group are well documented.⁴⁷ As seen in Fig. 3, the most intense band at 1989 cm^{-1} which is somewhat lower than the calculated value of 2040 cm^{-1} , corresponds to the NCS antisymmetric stretching mode and appears as a weak signal in the Raman spectrum, is very similar to that of acetyl isothiocyanate, for which the corresponding stretching mode is located at 1990 cm^{-1} .⁴² The most characteristic band, at 1733 cm^{-1} , can undoubtedly be attributed to the stretching mode of $\nu_{\text{C=O}}$. Additionally, the NCS bending mode was predicted at 459 cm^{-1} , which agrees very well with the observed band at 450 cm^{-1} in the IR spectrum of acetyl isothiocyanate.⁴² The C=C double bond stretching mode was calculated to have a relatively high IR intensity and Raman activity. This mode was observed at 1629 and 1622 cm^{-1} in the IR and Raman spectra, respectively. The absorption at 1406 cm^{-1} can be assigned to the deformation of the CH_2 group, and the absorptions at 1156 and 923 cm^{-1} are mainly the twist of the CH_2 group. $\text{CC}(\text{O})\text{N}$ out-of-plane bending is assigned to the band at 573 cm^{-1} . Other characteristic bands at 1233 and 711 cm^{-1} correspond to $\nu_{\text{C-C}}$ symmetrical stretching and $\nu_{\text{C-N}}$ stretching, which excludes the existence of acryloyl thiocyanate in our experiment.

Photoionization mass spectroscopy

The He I photoionization mass spectrum of $\text{CH}_2\text{CHC}(\text{O})\text{NCS}$ is shown in Fig. 4. The spectrum is relatively simple, showing five peaks: C_2H_3^+ , $\text{C}_2\text{H}_3\text{CO}^+$, NCS^+ , CONCS^+ and M^+ , with the dominant feature being the $\text{C}_2\text{H}_3\text{CO}^+$ peak, and is similar to that of acryloyl chloride.³⁹ Because there are no peaks for acryloyl chloride in Fig. 4 and no acryloyl chloride bands in the corresponding PE spectrum, it can be concluded that the $\text{C}_2\text{H}_3\text{CO}^+$ and C_2H_3^+ peaks are fragments of $\text{CH}_2\text{CHC}(\text{O})\text{NCS}$. Seen from the spectrum of $\text{CH}_2\text{CHC}(\text{O})\text{NCS}$, the parent ions are distinct, which indicates that this molecule is relatively stable under the experimental conditions. Four dissociation pathways can be envisaged: C_2H_3^+ ions with CONCS radicals, C_2H_3 radicals with CONCS^+ ions, $\text{C}_2\text{H}_3\text{CO}^+$ ions with NCS radicals and $\text{C}_2\text{H}_3\text{CO}$ radicals with NCS^+ ions. According to the intensity of the peaks in the spectrum, it is evident that the $\text{C}_2\text{H}_3\text{CO}^+$ ions with NCS radicals dissociation pathway is the dominant one for $\text{CH}_2\text{CHC}(\text{O})\text{NCS}$.

Photoelectron spectrum

Photoelectron spectroscopy with a He I resonance source (58.4 nm) is an effective method for investigating the electronic structure of unstable compounds and free radicals, in combination with *ab initio* calculations. The valence shell structure of molecules can be readily obtained by He I photoelectron energy analysis, especially when studying similar molecules. Previous photoelectron spectroscopic investigations on aromatic pseudohalides and acetyl pseudohalides have indicated that the first two occupied molecular orbitals (HOMOs) are the bonding- π and non-bonding- π orbitals of the NCS group. In addition, on energy grounds, it is expected that the $\text{NCS}-\pi$ delocalization/interaction will be more prominent in isothiocyanates than in isocyanates; this being due to the lower energy gap between the NCS and CO π -orbitals compared with NCO and CO π -orbitals. In alkyl derivatives, the relevant NCS bands are sharper than in aromatic examples, which supports the notion of stronger orbital mixing/interaction in the latter. These principles are of particular interest in connection with the present study.

As we know, within the He I energy region (21.2 eV), the non-bonding- and bonding- π levels (of the originally linear

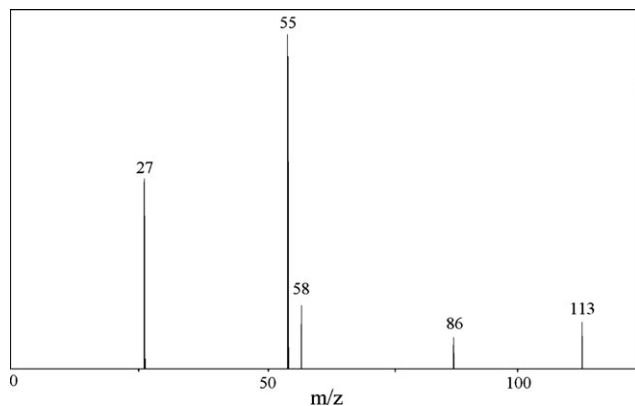


Fig. 4 The PIMS spectrum of $\text{CH}_2\text{CHC}(\text{O})\text{NCS}$.

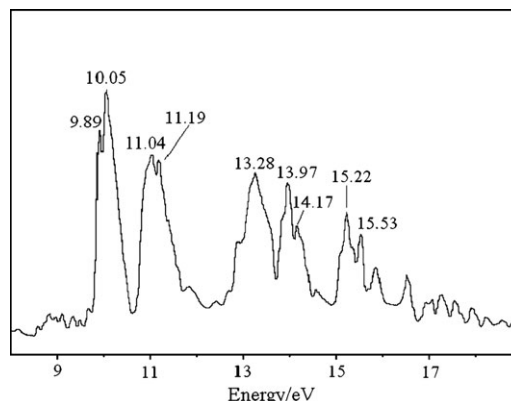


Fig. 5 The He I photoelectron spectrum of $\text{CH}_2\text{CHC}(\text{O})\text{NCS}$.

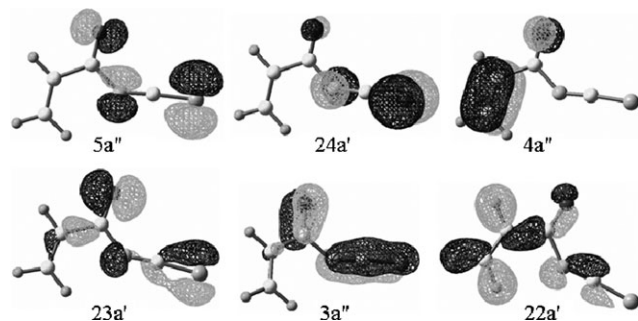
moieties) will give rise to four IPs in the linear molecule, viz. a'' (n.b.), a' (n.b.) and a'' (b), a' (b). One group of orbitals (with a' symmetry) lies in the molecular plane, while the other group (with a'' symmetry) belongs to orbitals perpendicular to the plane. These orbitals are partially localized on the pseudohalide carbonyl group and the $\text{C}=\text{C}$ bond. The information obtained from several empirical and theoretical considerations can be used simultaneously to assign the spectrum. The PE spectrum of $\text{CH}_2\text{CHC}(\text{O})\text{NCS}$ is depicted in Fig. 5. Before assigning the spectrum, ROVGF calculations (OVGF/6-311+G(d)) were carried out for the tc and cc conformers by using the structure parameters optimized at the B3LYP/6-311++G(3df,3pd) level to obtain the ionization energies. The experimental vertical ionization energies, calculated vertical ionization energies and molecular orbital characters of the tc and cc conformers of $\text{CH}_2\text{CHC}(\text{O})\text{NCS}$ are listed in Table 3. Drawings of six molecular orbitals (MOs) are shown in Fig. 6. Since tc and cc conformers with comparable energies are possible in some cases, first we should investigate whether the spectrum can originate from a mixture of both conformers or whether one of them dominates. However, in comparison to the calculated orbital energies, we have reduced our discussion to the analysis of the global minimum tc conformer.

As for the photoelectron spectrum of $\text{CH}_2\text{CHC}(\text{O})\text{NCS}$, nine distinct ionization bands were observed in the 10–18 eV region. The ionization energies of the different bands are in good agreement with the calculated values derived from the OVGF method. In addition, the photoelectron spectrum could be assigned by referring to the previously analyzed PE spectra of $\text{CH}_2\text{CHC}(\text{O})\text{Cl}$ and $\text{CH}_2\text{CHC}(\text{O})\text{NCO}$,³⁹ as well as its parent molecules, $\text{CH}_2\text{CHC}(\text{O})\text{H}$ ⁴⁸ and HNCS .¹⁸ The shape and intensity of the first two bands suggests that they should be attributed to two ionization processes. Consistent with analogous molecules HNCS ¹⁸ and $\text{CH}_3\text{C}(\text{O})\text{NCS}$,³⁵ and together with the analysis of the OVGF calculation results, these two bands are derived from $5a''$ and $24a'$, the components of which are bonding π -orbitals on the pseudohalide NCS moieties (primarily sulfur lone-pair electrons); the only difference between them is their orientation: the former is out-of-plane π_{NCS} , while the latter is in-plane π'_{NCS} . This is completely different to that of acryloyl isocyanate:³⁹ for the latter, the first occupied molecular orbital (HOMO) is mainly

Table 3 Experimental IP values, and IP values obtained by ROVGF/6-311 + G* calculations for the tc and cc conformers of CH₂CHC(O)NCS^{ab}

Experimental IP/eV	Calculated IP(tc)/eV	Calculated IP(cc)/eV	MO	Character
9.89	9.93 (0.89)	9.57 (0.90)	5a''	$\pi_{\text{N}=\text{C}=\text{S}}$
10.05	10.09 (0.89)	9.70 (0.90)	24a'	$\pi'_{\text{N}=\text{C}=\text{S}}$
11.04	11.01 (0.89)	10.69 (0.90)	4a''	$\pi_{\text{C}=\text{C}}$
11.19	11.14 (0.87)	11.27 (0.88)	23a'	$n_{\text{O}(\text{C}=\text{O})}$
13.28	13.40 (0.83)	13.16 (0.85)	3a''	$\pi_{\text{C}=\text{O}}, \pi_{\text{N}=\text{C}=\text{S}}$
13.97	13.76 (0.87)	13.45 (0.88)	22a'	$\sigma_{\text{C}=\text{C}}$
14.17	14.17 (0.85)	13.83 (0.87)	21a'	$\pi'_{\text{N}=\text{C}=\text{S}}$
15.22	15.44 (0.87)	15.23 (0.84)	20a'	$\pi_{\text{N}=\text{C}=\text{S}}$
15.53	15.51 (0.82)	15.25 (0.87)	2a''	$\pi_{\text{C}=\text{O}}, \pi_{\text{N}=\text{C}=\text{S}}$

^a Pole strength given in parentheses. ^b Geometry optimized at the B3LYP/6-311++ G(3df,3pd) level of approximation.

**Fig. 6** Drawings of selected occupied MOs of CH₂CHC(O)NCS.

the C=C π -orbital. This may be caused by the small energy gap between the NCS and the C=O π -orbital compared with that between the NCO and the C=O π -orbital, which also results in the shift of the first vertical ionization of CH₂CHC(O)NCS to a lower energy. An interesting and important feature of the PE spectra of compounds containing SCN is that the energetic order of the two highest occupied orbitals is $\pi(a'') < \pi(a')$, such as for HNCS,¹⁸ CH₃NCS¹⁸ and CH₃C(O)NCS.³⁵ The separation of the $\pi(a'')$ and $\pi(a')$ is also quite narrow, which indicates that the interaction between the π_{NCS} and $\pi_{\text{C=O}}$ is strong. The same phenomenon occurs in CH₂CHC(O)NCS, where the separation of the first two bands is only 0.16 eV.

Further calculations (UB3LYP/6-311++G(3df, 3pd)) were performed in order to analyze the nature of the radical cation formed in the first ionization process. The results demonstrate that the atomic charges are delocalized over the whole molecule, with an appreciable fraction localized on the carbonyl oxygen atom and the sulfur atom (Table 4). The optimized structural parameters of the radical cation are summarized in Table 2. In a similar way, the C–N and C=O bond lengths and the O=C–N bond angle are the geometric parameters most influenced by ionization. The planar form, with a *trans* orientation of the C=C and C=O bonds, is

changed after ionization. These results agree with a picture of electron ionization mainly localized on the NCS group, with a reinforced bond character in the C=C and C=O bonds, and a decrease in the corresponding C–N and C=S bonds. The planar structure of the neutral molecule changed after the first ionization process, and this change in geometry may be the reason for the structureless broad band observed when the first ionization process occurs. A value of $\text{IP}^{\text{ad}} = 9.57$ eV is derived from the difference between the energies of the neutral and the radical cation form.

The next two bands, which overlap with each other, come from the ionization of the 4a'' and 23a' orbitals. Combining our calculated OVGF results and the assignments of the PE spectra of other RNCS molecules, we have assigned the third band at 11.04 eV as arising from the ionization of the out-of-plane bonding $\pi_{\text{C}=\text{C}}$ -orbital and the fourth band at 11.19 eV as arising from the ionization of the in-plane carbonyl oxygen lone pair n_{O} -orbital. These bands are in good agreement with the calculated values of 11.01 and 11.14 eV, respectively. Compared with CH₂CHC(O)NCO,³⁹ the ionization of the bonding $\pi_{\text{C}=\text{C}}$ shifts to a higher energy by 0.36 eV.

The PE band at 13.28 eV is the ionization of the 3a'' orbital, which is in agreement with the calculated 13.40 eV value. The primary MO character is bonding- $\pi_{\text{C=O}}$ with a considerable contribution from the non-bonding- π_{NCS} . Similar bands occur in the PE spectrum of CH₃C(O)NCS (13.04 eV) {4a''($\pi_{\text{C=O}}, \pi_{\text{NCS}}$)}.³⁵ The sixth band at 13.97 eV, which originates from the ionization of the 22a' orbital, has a main character of $\sigma_{\text{C}=\text{C}}$. With the help of theoretical calculations, the next two bands at 14.17 and 15.22 eV are assigned to the ionization of the 21a' and 20a' orbitals, the main characters of which are same as each other, both arising from in-plane π'_{NCS} . The distinct band in the PE spectrum of CH₂CHC(O)NCS at 15.53 eV is tentatively assigned to the out-of-plane π MO (2a''), with a primary contribution of $\pi_{\text{C=O}}$ and π_{NCS} characters, and is in good agreement with the calculated value of 15.51 eV. The bands in the higher

Table 4 Atomic charge for the neutral and radical cation forms of CH₂CHC(O)NCS, calculated by the UB3LYP/6-311++ G(3df,3pd) approximation

Atom ^a	C1	C2	H3	H4	H5	C6	O7	N8	C9	S10	TAC ^b
CH ₂ =CHC(O)NCS	−0.214	0.342	0.045	0.026	0.036	0.797	−0.681	−0.856	0.642	−0.136	0
CH ₂ =CHC(O)NCS ⁺	−0.094	0.438	0.079	0.028	0.057	0.855	−0.513	−0.801	0.757	0.195	1
Δq^c	0.120	0.096	0.034	0.002	0.021	0.058	0.168	0.055	0.115	0.331	1

^a For atom numbering, see Fig. 2. ^b TAC = total atomic charge. ^c $\Delta q = q_{\text{CH}_2=\text{CHC(O)NCS}^+} - q_{\text{CH}_2=\text{CHC(O)NCS}}$

Table 5 Natural bond orbital analysis for CH₂CHC(O)NCO and CH₂CHC(O)NCS with the B3LYP method at the 6-311++G(3df,3pd) basis set level^a

	Donor NBO	Acceptor NBO	$E^{(2)}/\text{kcal mol}^{-1}$
CH ₂ =CHC(O)NCO	LP(1)O ₁₀	$\pi^*(1)\text{N}_8\text{-C}_9$	11.86
CH ₂ =CHC(O)NCS	LP(1)S ₁₀	$\pi^*(1)\text{N}_8\text{-C}_9$	18.79

^a For atom numbering, see Fig. 2.

ionization energy region of the spectrum over 16.0 eV are broad features, making it difficult to make further assignments.

Relative reactivity

It has been found that substituents do not significantly affect the electron density of NCX groups.^{6,35,49} The chemical reactivity of the NCX group is based on nucleophilic attack on the electron deficient carbon, which can be rationalized by simple resonance structures. $\text{R-N}=\text{C}=\text{X}$ (I) \leftrightarrow $\text{R-N}^--\text{C}^+=\text{X}$ (II) \leftrightarrow $\text{R-N}=\text{C}^+-\text{X}^-$ (III) (X = O or S). This is in accordance with our population analysis (see the ESI, Table S2†), which shows that the NCX carbon always has a positive partial charge. The results of a natural population analysis show that the atomic charges in CH₂CHC(O)NCS are C: +0.25, N: −0.53 and S: +0.09, and in NCO derivatives are C: +0.91, N: −0.65 and O: −0.45. However, in isothiocyanates, since the carbon's partial charge is considerably smaller, they can be expected to be less reactive than their isocyanate analogues. In addition, a natural bond orbital (NBO) analysis also supports this notion: the delocalization energy of the p-type lone pair of sulfur to the $\pi^*(\text{N-C})$ orbital is 18.79 kcal mol^{−1}, which is bigger than that of the p-type lone pair of oxygen to the $\pi^*(\text{N-C})$ orbital (11.86 kcal mol^{−1}) (see Table 5). Furthermore, the ionization energy of the electron deficient NCX orbital may be an indicator of chemical reactivity; the higher the ionization energy (*i.e.* the lower the NCX orbital energy) the more stable the intermediate will be. Our investigations on the electronic structure of CH₂CHC(O)NCS may have further implications on understanding its chemical reactivity.

Conclusions

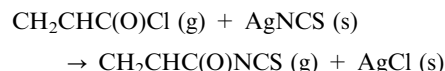
Acryloyl isothiocyanate, CH₂CHC(O)NCS, was synthesized by a heterogeneous reaction between acryloyl chloride and AgNCS, and was investigated by He I photoelectron spectroscopy, photoionization mass spectroscopy, IR and Raman spectroscopy, and theoretical calculations. The results show that the most stable conformer of CH₂CHC(O)NCS is the *tc* (*trans-cis*) form: with the C=C bond in a *trans* orientation with respect to the C=O bond, and the C=O bond in a *cis* orientation with respect to the NCS group. The first vertical ionization potential of CH₂CHC(O)NCS is at 9.89 eV. In order to understand the nature of the first ionization processes, the radical cation form of CH₂CHC(O)NCS was also studied. It was found that its structure changed after ionization. Comparing CH₂CHC(O)NCS with its isocyanate analogue, the main characters of their HOMOs are different; the first ionization of the former originates from the out-of-plane

bonding π_{NCS} orbital, while that of the latter originates from the bonding $\pi_{\text{C}=\text{C}}$ orbital. The adiabatic energy is 9.57 eV, which is not identical to the first vertical ionization energy according to Frank–Condon principle. Furthermore, NPA and NBO analyses combined with electronic structural investigations showed that the reactivity of CH₂CHC(O)NCS is less than that acryloyl isocyanate in nucleophilic reactions.

Experimental section

Experimental and theoretical methods

CH₂CHC(O)NCS is typically prepared by the reaction of acryloyl chloride with ammonium thiocyanate⁵⁰ or potassium thiocyanate⁵¹ in dioxane. However, in this paper, it was synthesized quantitatively by a new and convenient gas–solid reaction between acryloyl chloride and AgNCS for 48 h at a room temperature of 20 °C. Under these conditions, the volatile product was slowly pumped and separated by trap-to-trap condensation to remove the minor impurity of acryloyl chloride. The final purity was checked by IR and mass spectroscopy. The reaction equation is as follows:



IR and Raman spectroscopy

IR spectra, recorded at 4 cm^{−1} resolution, were collected on a Thermo Nicolet 6700 interferometer equipped with a 20 cm single-pass gas cell. The cell, with KBr windows, gave a spectral range from 4000 to 400 cm^{−1}. All compounds had sufficient vapor pressure and were pumped continuously through the cell using a rotary pump. Raman signals were collected and focused into a spectrometer (SpectraPro-500i, Acton) equipped with a liquid nitrogen cooled CCD detection system (SPEC-10-400B/LbN, Roper Scientific). The sample in a 4 mm glass capillary was excited with a 200 mW Ar⁺ laser at 488 nm (Spectra-Physics Beam Lock).

Photoelectron spectroscopy

PE spectra were recorded on a double-chamber UPS-II instrument designed specifically to detect transient species at a resolution of ≈ 30 meV, as indicated by the Ar⁺(²P_{2/3}) photoelectron band.^{52,53} Experimental vertical ionization energies (IP in eV) were calibrated by the simultaneous addition of a small amount of argon and methyl iodide to the sample. Mass analysis of ions was achieved by a time-of-flight mass analyzer mounted directly at the photoionization point. Ionization was provided by single wavelength He I radiation. PE and PIMS spectra, although not measured simultaneously, were recorded within seconds of each other under identical conditions; thus, it was assumed that for a given PE spectrum, the subsequent PIMS spectrum was of the same compound.

Quantum chemical calculations

Electronic structure calculations were carried out using the Gaussian series of programs.⁵⁴ Because the values and order of molecular orbital (MO) energies depends on molecular

geometry, the geometries of the neutral ground state and lowest-lying cationic state of $\text{CH}_2\text{CHC}(\text{O})\text{NCS}$ were optimized using density functional theory (B3LYP, B3P86 and B3PW91) at the 6-311++G(3df,3pd) basis set level. The single point energy of different conformers were calculated by the *ab initio* (MP2) method with the 6-311++G** basis set. Density functional calculations were previously employed for pseudohalides and had a good performance.^{55,56} The vibrational frequencies were computed analytically and zero-point energy (ZPE) corrections were included in the calculation of relative energies. To assign the PE spectra, out-valence Green's function (OVGF/6-311+G(d)) calculations, which include sophisticated correlation effects of the self-energy, were applied to the most stable conformer of each compound to give accurate results of the vertical ionization energies. The adiabatic energy was obtained according to the energy differences between the most stable conformer and the corresponding radical cation form. Mulliken population analysis was applied to assign the charges of both the neutral and radical cation forms. Three-dimensional MO plots were obtained by using the Gauss View program with a 0.06 isodensity.

Acknowledgements

This project was supported by the Knowledge Innovation Program (Grant no. KZCX2-YW-205) of the Chinese Academy of Sciences, the 973 program (no. 2006CB403701) and the 863 program (no. 2006AA06A301) of the Ministry of Science and Technology of China, and the National Natural Science Foundation of China (Contract no. 20673123).

References

- B. A. Trofimov, *J. Heterocycl. Chem.*, 1999, **36**, 1469.
- M. Avalos, R. Babiano, P. Cintas, J. L. Jimenez and J. C. Palacios, *Heterocycles*, 1992, **33**, 973.
- A. K. Mukerjee and R. Ashare, *Chem. Rev.*, 1991, **91**, 1.
- S. A. Mayekar and V. V. Mulwad, *Indian J. Chem., Sect. B: Org. Chem. Incl. Med. Chem.*, 2008, **47**, 1254.
- J. R. Durig, G. A. Guirgis, K. A. Krutules, H. V. Phan and H. D. Stidham, *J. Raman Spectrosc.*, 1994, **25**, 221.
- I. Novak and B. Kovac, *J. Phys. Chem. A*, 2003, **107**, 2743.
- T. Sultana and G. P. Savage, *Proc. Nutr. Soc. N. Z.*, 2003, **28**, 126.
- R. Wong and S. J. Dolman, *J. Org. Chem.*, 2007, **72**, 3969.
- A. Papadopoulos and P. Alderson, *Ann. Appl. Biol.*, 2007, **151**, 61.
- Y. S. Keum, W. S. Jeong and A. N. T. Kong, *Drug News Perspect.*, 2005, **18**, 445.
- Y. Zhang, S. Yao and J. Li, *Proc. Nutr. Soc.*, 2006, **65**, 68.
- M. Traka and R. Mithen, *Phytochem. Rev.*, 2008, **1**, 269.
- S. S. Hecht, *J. Nutr.*, 1999, **129**, 768S.
- R. Sommerlade, P. Ekici and H. Parlar, *Atmos. Environ.*, 2006, **40**, 3306.
- P. W. Ayers, J. S. M. Anderson and L. J. Bartolotti, *Int. J. Quantum Chem.*, 2005, **101**, 520.
- T. Veszpremi, T. Pasinszki and M. Feher, *J. Chem. Soc., Faraday Trans.*, 1991, **87**, 3805.
- B. J. M. Neijzen and C. A. De Lange, *J. Electron Spectrosc. Relat. Phenom.*, 1980, **18**, 179.
- S. Craddock, E. A. V. Ebsworth and J. D. Murdoch, *J. Chem. Soc., Faraday Trans. 2*, 1972, **68**, 86.
- I. Tokue, A. Hiraya and K. Shobatake, *Chem. Phys.*, 1987, **117**, 315.
- E. Cortes, M. F. Erben, M. Geronces, R. M. Romano and C. O. Della Vedova, *J. Phys. Chem. A*, 2009, **113**, 564.
- T. Veszpremi, T. Pasinszki, L. Nyulaszi, G. Csonka and I. Barta, *J. Mol. Struct.*, 1988, **175**, 411.
- D. C. Frost, C. B. MacDonald, C. A. McDowell and N. P. C. Westwood, *J. Am. Chem. Soc.*, 1981, **103**, 4423.
- M. A. King and H. W. Kroto, *J. Am. Chem. Soc.*, 1984, **106**, 7347.
- C. I. Beard and B. P. Dailey, *J. Chem. Phys.*, 1950, **18**, 1437.
- R. G. Lett and W. H. Flygare, *J. Chem. Phys.*, 1967, **47**, 4730.
- C. G. Overberger and H. A. Friedman, *J. Org. Chem.*, 1965, **30**, 1926.
- P. Rosmus, H. Stafast and H. Bock, *Chem. Phys. Lett.*, 1975, **34**, 275.
- R. J. Richards, R. W. Davis and M. C. L. Gerry, *J. Chem. Soc., Chem. Commun.*, 1980, 915.
- K. Banert, M. Hagedorn and A. Müller, *Eur. J. Org. Chem.*, 2001, 1089.
- G. Jonkers, R. Mooyman and C. A. De Lange, *Mol. Phys.*, 1981, **43**, 655.
- Y. M. Li, Z. M. Qiao, Q. Sun, J. C. Zhao, H. Y. Li and D. X. Wang, *Inorg. Chem.*, 2003, **42**, 8446.
- L. Du, L. Yao and M. F. Ge, *Eur. J. Inorg. Chem.*, 2007, 4514.
- D. C. Frost, H. W. Kroto, C. A. McDowell and N. P. C. Westwood, *J. Electron Spectrosc. Relat. Phenom.*, 1977, **11**, 147.
- D. C. Frost, C. B. Macdonald, C. A. McDowell and N. P. C. Westwood, *Chem. Phys.*, 1980, **47**, 111.
- X. Q. Zeng, L. Yao, M. F. Ge and D. X. Wang, *J. Mol. Struct.*, 2006, **789**, 92.
- C. P. Ma and M. F. Ge, *J. Mol. Struct.*, 2008, **892**, 68.
- S. T. Vallejos, M. F. Erben, H. Willner, R. Boese and C. O. Della Vedova, *J. Org. Chem.*, 2007, **72**, 9074.
- J. E. Katon and W. R. Fearheller, Jr., *J. Chem. Phys.*, 1967, **47**, 1248.
- M. F. Ge, C. P. Ma and W. Xue, *J. Phys. Chem. A*, 2009, **113**, 3108.
- H. M. Badawi and W. Forner, *J. Mol. Struct. (THEOCHEM)*, 2001, **535**, 103.
- J. R. Durig, R. J. Berry and P. Groner, *J. Chem. Phys.*, 1987, **87**, 6303.
- J. R. Durig, G. A. Guirgis and K. A. Krutules, *J. Mol. Struct.*, 1994, **328**, 97.
- H. M. Badawi, W. Forner and Z. S. Seddigi, *J. Mol. Struct. (THEOCHEM)*, 2003, **631**, 127.
- A. P. Scott and L. Radom, *J. Phys. Chem.*, 1996, **100**, 16502.
- G. Rauhut and P. Pulay, *J. Phys. Chem.*, 1995, **99**, 3093.
- J. R. Durig, M. R. Jalilian and J. F. Sullivan, *J. Raman Spectrosc.*, 1981, **11**, 459.
- C. W. Gullissou and J. R. Nielsen, *J. Mol. Spectrosc.*, 1957, **1**, 158.
- A. Katrib and J. W. Rabalais, *J. Phys. Chem.*, 1973, **77**, 2358.
- M. F. Erben and C. O. Della Vedova, *Inorg. Chem.*, 2002, **41**, 3740.
- F. A. Ei-Saied, S. H. Ei-Hamouly and O. A. Mansour, *Pol. J. Chem.*, 1994, **68**, 1937.
- A. P. Sineokov and M. E. Sergeeva, *J. Org. Chem. USSR (Engl. Transl.)*, 1967, **3**, 1427.
- X. Q. Zeng, M. F. Ge, Z. Sun and D. X. Wang, *Inorg. Chem.*, 2005, **44**, 9283.
- C. P. Ma, X. Q. Zeng and M. F. Ge, *J. Mol. Struct.*, 2008, **875**, 143.
- M. J. Frisch, G. W. Trucks, H. B. Schlegel, G. E. Scuseria, M. A. Robb, J. R. Cheeseman, J. A. Montgomery Jr, T. Vreven, K. N. Kudin, J. C. Burant, J. M. Millam, S. S. Iyengar, J. Tomasi, V. Barone, B. Mennucci, M. Cossi, G. Scalmani, N. Rega, G. A. Petersson, H. Nakatsuji, M. Hada, M. Ehara, K. Toyota, R. Fukuda, J. Hasegawa, M. Ishida, T. Nakajima, Y. Honda, O. Kitao, H. Nakai, M. Klene, X. Li, J. E. Knox, H. P. Hratchian, J. B. Cross, C. Adamo, J. Jaramillo, R. Gomperts, R. E. Stratmann, O. Yazyev, A. J. Austin, R. Cammi, C. Pomelli, J. W. Ochterski, P. Y. Ayala, K. Morokuma, G. A. Voth, P. Salvador, J. J. Dannenberg, V. G. Zakrzewski, S. Dapprich, A. D. Daniels, M. C. Strain, O. Farkas, D. K. Malick, A. D. Rabuck, K. Raghavachari, J. B. Foresman, J. V. Ortiz, Q. Cui, A. G. Baboul, S. Clifford, J. Cioslowski, B. B. Stefanov, G. Liu, A. Liashenko, P. Piskorz, I. Komaromi, R. L. Martin, D. J. Fox, T. Keith, M. A. Al-Laham, C. Y. Peng, A. Nanayakkara, M. Challacombe, P. M. W. Gill, B. Johnson, W. Chen, M. W. Wong, C. Gonzalez and J. A. Pople, *GAUSSIAN 03 (Revision B.03)*, Gaussian, Inc., Pittsburgh, PA, 2003.
- W. G. Wang, L. Yao, X. Q. Zeng, M. F. Ge, Z. Sun, D. X. Wang and Y. H. Ding, *J. Chem. Phys.*, 2006, **125**, 6.
- W. G. Wang, M. F. Ge, L. Yao, X. Q. Zeng, Z. Sun and D. X. Wang, *ChemPhysChem*, 2006, **7**, 1382.